Research in Veterinary Science 203 (2026) 106121

Contents lists available at ScienceDirect

Research in Veterinary Science

journal homepage: www.elsevier.com/locate/rvsc

A standardized osteometric method for identifying Iberian raptors from skeletal remains

Andrea Miguel-Batuecas [a,1], Juan A. De Pablo-Moreno [b,c,1], Manuel Fuertes-Recuero [c,d], Ariana Fuentes-Díaz [c], Fernando González [e,f], Laura Suárez [e,g], Victoriano García-Matarranz [h], Luis Revuelta [c,*]

[a] Department of Genetics, Physiology and Microbiology, School of Biological Sciences, Complutense University, Madrid, Spain
[b] Department of Veterinary Sciences, School of Biomedical and Health Sciences, Universidad Europea de Madrid, Villaviciosa de Odón, Spain
[c] Department of Physiology, School of Veterinary Medicine, Complutense University, Madrid, Spain
[d] Veterinary Teaching Hospital, Complutense University of Madrid, Madrid, Spain
[e] GREFA (Grupo de Rehabilitación de la Fauna Autóctona y su Hábitat), Majadahonda, Madrid, Spain
[f] Departmental Section of Pharmacology and Toxicology, School of Veterinary Medicine, Complutense University, Madrid, Spain
[g] Departmental Section of Anatomy and Embriology, School of Veterinary Medicine, Complutense University of Madrid, Madrid, Spain
[h] Conservation Action Area, Spanish Ministry of Ecological Transition and the Demographic Challenge, Madrid, Spain

ARTICLE INFO

Keywords:
Measurements
Raptors
Identification
Canonical analysis
Conservation

ABSTRACT

Raptors suffer high mortality rates due to anthropogenic threats, such as electrocution from power lines or lead poisoning, so the specific identification of skeletal remains is essential for establishing monitoring and protection programmes.

This study developed and validated a standardized osteometric method for measuring long bones and craniopelvic bones from skeletal remains to identify raptor species. A database of 26 species of Iberian raptors (n = 853) was developed based on 11 measurements of 9 bones, including the ulna, sternum, femur, humerus, tarsometatarsus, tibiotarsus, and radius, as well as the synsacrum length and postacetabular ilium width and length and width of the skull. Missing values were estimated using multiple linear regression, and canonical discriminant analysis was applied to correct and modify the databases. Cross-validation was added to this analysis. Additionally, the obtained model was verified using external radiographs.

The highest percentage of success was obtained with the tarsometatarsus-ulna combination (94.53%), followed by tarsometatarsus-radius (94.05%) and tarsometatarsus-humerus (93.02%), when two bone lengths were combined. When a third measurement was incorporated, the tarsometatarsus-ulna-femur combination achieved a 99.45% correct classification rate. In blind verification testing, the radiographs of 15 individuals, the tarsometatarsus-ulna model correctly classified all samples, achieving a 100% success rate. These results show that the study method provides a simple and replicable protocol for identifying raptor species from incomplete skeletal remains. This optimizes the monitoring of mortality and supporting conservation measures.

1. Introduction

Raptors are a diverse group of birds belonging to several orders, including *Accipitriformes* (eagles, ospreys, harriers, kites, hawks, and Old World vultures, such as griffon and cinereous vulture, bearded, and Egyptian vultures; *Falconiformes* (falcons and caracaras); and *Strigiformes* (owls, including barn and little owls) (McClure et al., 2018, 2022; Vidaña et al., 2020). Although birds of prey represent approximately 5% of all birds, they play a fundamental ecological role in maintaining ecosystem balance. As top predators, they regulate prey populations, contribute to nutrient recycling through scavenging, and serve as indicators of biodiversity health (Donázar et al., 2016; Santangeli and Girardello, 2021). Despite their ecological importance, many raptor species are classified as vulnerable or endangered due to small population sizes and low reproductive rates, leading to global declines (McClure et al., 2018, 2023). Their high trophic position and generally

* Corresponding author.
E-mail address: lrevuelt@ucm.es (L. Revuelta).
[1] These authors have contributed equally as first authors.

https://doi.org/10.1016/j.rvsc.2026.106121
Received 3 November 2025; Received in revised form 18 January 2026; Accepted 22 February 2026
Available online 23 February 2026

slow reproductive rates make them particularly susceptible to human-caused threats, raising major conservation concerns worldwide (Buechley and Şekercioğlu, 2016).

Raptor mortality from natural causes is usually related to age, meteorological phenomena (e.g., storms, extreme temperatures, and strong winds), diseases (e.g., West Nile virus and infected prey), and predation (e.g., intraspecific and interspecific competition) (Dwyer et al., 2016; Komosa et al., 2018; Vidaña et al., 2020). However, the factor currently posing the greatest threat to their conservation is the increase in human activities worldwide (Santangeli and Girardello, 2021). The most frequent threats include habitat loss from intensive agriculture, deforestation, and illegal hunting. Still, the most significant threats are poisoning (rodenticides, lead, and pesticides), collisions with anthropogenic infrastructures, and electrocution from power lines and energy installations such as wind turbines and solar panels (Berny et al., 2015; Descalzo et al., 2021; Estellés-Domingo and López-López, 2025; O'Bryan et al., 2022; Rial-Berriel et al., 2021; Vyas et al., 2022). Lead poisoning is the most widespread form of intoxication in birds of prey, as they are particularly exposed to bullet or pellet residues when consuming carcasses (Katzner et al., 2024). Similarly, global access to electricity has made collisions with overhead wires and electrocutions on high-voltage towers significant causes of mortality (Gómez-Catasús et al., 2020; Guil and Pérez-García, 2022; Tincher et al., 2020). Despite the implementation of mitigation such as insulation, visual markers, and increased distance between towers, the rate of electrocution and collision mortality remains elevated, underscoring the need to optimize all strategies (Eccleston and Harness, 2018).

The discovery and identification of skeletal remains beneath power lines, wind farms, and protected areas provides an opportunity to determine which species are most affected and to estimate mortality rates. This information is crucial for developing appropriate protection plans for each species (Estellés-Domingo and López-López, 2025; Guil and Pérez-García, 2022). Traditionally, bird carcasses have been identified based on geographic location and season, supplemented by analyses of morphological and plumage characteristics typical of each species in both juvenile and adult specimens, as well as in males and females, and by DNA analysis (Dalén et al., 2017; Sarasola et al., 2018; Woodward, 2023). However, identifying some individuals or species can be difficult due to factors such as decomposition, absence of plumage, damage by other scavenger species, and incomplete skeletal remains (Gómez-Catasús et al., 2020). Identification based on osteometric measurements and bone morphology is uncommon because no standardized method has been established, limiting the applicability of this approach. Nevertheless, several studies have used osteological collections to identify different species using bones or archaeological remains (Gorobets et al., 2024; Watson and Ledogar, 2019). Some studies have used osteometry to examine variations in bone structure (Singh et al., 2015), determine sex (Analla et al., 2022), and develop identification guides for raptors (García-Matarranz, 2019).

A standardized osteometric method would be highly valuable for forest rangers, field technicians, and personnel training in wildlife environmental conservation. In contexts where only fragmented, poorly preserved, or incomplete skeletons are available, the measurement of a single bone or a combination of bones could enable reliable species identification. Given the current lack of standardized protocols for identifying skeletal remains, this study aimed to develop a reliable method for identifying birds of prey based on osteometric data. The goal was to determine the most effective combination of bone measurements for predicting species, which would facilitate population monitoring, assess anthropogenic impact, and implement more effective conservation strategies.

2. Materials and methods

2.1. Data

A retrospective study was performed using a database of bone measurements from the research group (Ref. M-004841/2021) (Supplementary Table 1). The database comprises 853 individuals representing 26 species of Iberian raptors. For each species, nine bones were measured for a total of 11 different measurements. In accordance with previously described protocols, measurements included the lengths of the ulna, radius, humerus (Fig. 1). femur, tarsometatarsus, tibiotarsus (Fig. 2), and sternum, plus the synsacrum length and postacetabular ilium width and the length and width of the skull (Fig. 3) (García-Matarranz, 2019). For measurements up to 200 mm, a digital caliper with 0.01 mm precision was used; however, measurements were recorded to the nearest 0.1 mm. For measurements between 200 and 330 mm, an analogue depth caliper with 0.1 mm precision was used. For measurements exceeding 330 mm, a measuring tape with 1 mm precision was used. The number of individuals per species included in the database is shown in Table 1. However, not all individuals had measurements for all bones because there were skeletal remains.

2.2. Statistical analysis

2.2.1. Estimation of missing values

Estimation of missing values was performed using multiple linear regression with the MVA (Missing Value Analysis) function in IBM® SPSS® Statistics (Version 25; IBM Corporation, Armonk, New York, USA), since not all 11 bone measurements were available for all individuals. This function estimates missing values based on the relationships between available variables in each case.

2.2.2. Canonical discriminant analysis

A canonical discriminant analysis was performed using the SAS® statistical program (Version 9.4; Cary, North Carolina, USA) to predict a categorical variable (species) from continuous independent variables

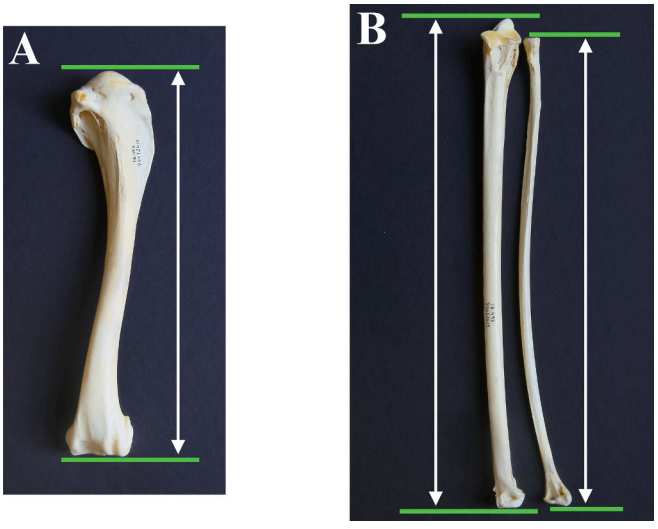

Fig. 1. Reference points for osteometric measurements of the forelimb bones in the Cinereous vulture (*Aegypius monachus*). (A) Humerus length (white arrow): from the humeral head to the ventral condyle. (B) Ulna length (left; white arrow): from the olecranon to the distal end of the ulna; radius length (right; white arrow): from the proximal to the distal end of the radius.

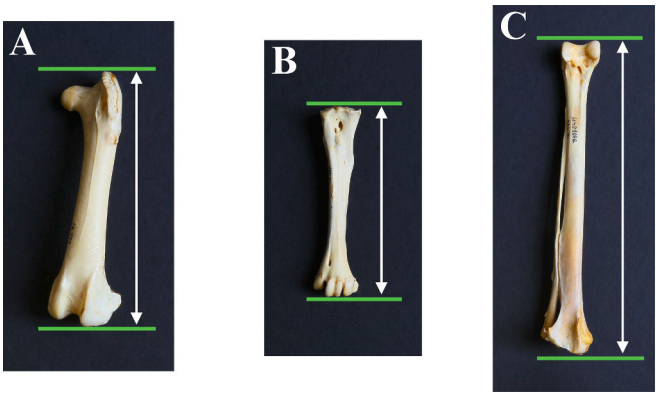

Fig. 2. Reference points for osteometric measurements of the hind limb bones in the Cinereous vulture (*Aegypius monachus*). (A) Femur length (white arrow): from the distal end of the trochanteric crest to the lateral condyle. (B) Tarsometatarsus length (white arrow): from the medial hypotarsal crest to the middle trochlea. (C) Tibiotarsus length (white arrow): from the cranial cnemial crest to the distal end of the medial condyle.

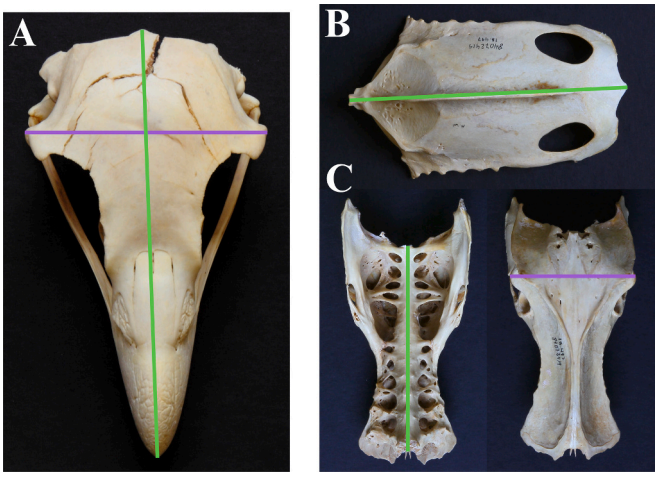

Fig. 3. Reference points for osteometric measurements of the head bone (skull, A) and trunk bones (sternum, B, and pelvis, C) in the Cinereous vulture (*Aegypius monachus*). (A) Skull length (green line): from the tip of the premaxilla to the cerebellar protuberance; skull width (purple line): from the right postorbital process to the left postorbital process. (B) Sternum length (green line): from the tip of the cranial spine (or rostrum) to the midpoint of the distal crest, measured along the ventral surface. (C) synsacrum lengthlength (left, green line): from the cranial to the caudal end of the synsacrum; postacetabular ilium width (right, purple line): from the right to the left postacetabular dorsolateral crest of the ilium at the point of maximum width. (For interpretation of the references to colour in this figure legend, the reader is referred to the web version of this article.)

(bone measurements). This analysis generated linear functions that maximised interspecies variation, resulting in canonical variables.

A data matrix, M (pnk), was used for this purpose, where p corresponds to the number of bone measurements recorded, n to the number of individuals, and k to the number of species included in the analysis. The resulting linear functions were expressed as:

$$\mathrm{CVAi} = \mathrm{ai1\ m1} + \mathrm{ai2\ m2} + \mathrm{ai3\ m3} + \ldots + \mathrm{aip\ mp},$$

where i is the number of linear functions, aip are the canonical coefficients indicating the partial contribution of each bone measurement to the discriminant function, and m_i are the different bone measurements used (Sorbolini et al., 2016).

Once the database was completed, this analysis was performed using

Table 1
Names and numbers of individuals per species from raw data.

Scientific Name	Common Name	Individuals
Accipiter gentilis	Goshawk	34
Accipiter nisus	Sparrowhawk	34
Aegypius monachus	Cinereus vulture	49
Aquila adalberti	Imperial eagle	46
Aquila chrysaetos	Golden eagle	47
Aquila fasciata	Bonelli's eagle	60
Bubo bubo	Eagle owl	27
Buteo buteo	Common buzzard	34
Circaetus gallicus	Short-toed snake eagle	22
Circus aeruginosus	Western marsh harrier	31
Circus cyaneus	Hen harrier	10
Circus pygargus	Montagu's harrier	31
Elanus caerulus	Black-winged kite	15
Falco columbarius	Merlin	17
Falco naumanni	Lesser kestrel	27
Falco peregrinus	Peregrine falcon	33
Falco subbuteo	Eurasian hobby	25
Falco tinnunculus	Common kestrel	34
Gypaetus barbatus	Bearded vulture	15
Gyps fulvus	Griffon vulture	52
Hieraaetus pennatus	Booted eagle	34
Milvus migrans	Black kite	49
Milvus milvus	Red kite	40
Neophron percnopterus	Egyptian vulture	36
Pandion haliaetus	Osprey	24
Pernis apivorus	Honey buzzard	27
Total:		853

estimated values obtained by multiple linear regression and comparing the 11 osteometric variables with one another. If corrections to the original database were required, the analysis would be rerun, potentially altering the number of variables included.

2.2.3. Cross-validation for species identification

Following canonical discriminant analysis, cross-validation was performed to assess the relationship among bone measurements for which only one measurement was available (length of the ulna, sternum, femur, humerus, tarsometatarsus, tibiotarsus, and radius) and bones with two available measurements (synsacrum length and postacetabular ilium width and length and width of the skull) with the rest of the bones. Cross-validation was performed using the models obtained from the canonical discriminant analysis to calculate the error rate —the number of individuals incorrectly classified by the program with respect to the original database. The error percentage was then converted into an accuracy percentage, representing the probability of correctly classifying an individual within its species based on two bone measurements. Additionally, canonical discriminant analysis and cross-validation were repeated using the model that achieved the highest classification accuracy. This model was subsequently compared with those derived from the remaining bone measurements to maximise accuracy, approaching 100% whenever possible.

2.3. Verification of the identifying method by bone measurements using radiographs

Radiographs from 15 individuals not included in the study were used to verify the accuracy of the identification method. These radiographs corresponded to four species: *Falco tinnunculus* ($n = 4$), *Accipiter nisus* (n = 4), *Pernis apivorus* ($n = 3$), and *Falco peregrinus* (n = 4). To minimize potential bias, the person performing the measurements was blinded to species identity during the procedure; species information recorded in the clinical records was consulted only after the analysis to verify the results. All radiographs were provided by The Wildlife Hospital of the Rehabilitation Group for Native Wildlife and its Habitat (GREFA; Madrid, Spain). Ginkgo CADx program (version 3.7.1.1573.41 bits; MetaEmotion S.L., Valladolid, Spain) was used to measure bone lengths.

All measurements were taken using the same anatomical landmarks as those employed to build the reference database (García-Matarranz et al., 2013; García-Matarranz, 2019). Both measurements and canonical discriminant analysis were performed under blind study conditions, and the species of each specimen was unknown in all cases.

3. Results

3.1. First prediction

The original database (Supplementary Table 1) included 853 individuals from 26 Iberian raptor species, of which 378 had incomplete data. Therefore, an estimation analysis was performed on the database to complete the missing measurements. Once the database was completed (Supplementary Table 2), a canonical discriminant analysis was performed to compare 11 bone measurements from nine bones (ulna, sternum, femur, humerus, tarsometatarsus, tibiotarsus, radius, pelvis, and skull) across individuals of different species. The aim was to predict each individual's specific membership and assess whether their classification matched the original identification.

This analysis revealed several discrepancies between the predicted and original species classifications. Therefore, the original database was reviewed in collaboration with personnel from MITECO, who had been responsible for the sampling process. Several classification errors were detected during this review of the initial.

Individuals No. 13 and No. 39, initially classified as *Milvus milvus*, were subsequently reclassified as *Milvus migrans* after identification of sampling errors. Individual No. 154, registered as *Bubo bubo*, had an erroneous skull width measurement, which was removed, allowing the rest to be re-estimated. Individuals No. 555 and No. 570, first classified as *Circus pygargus*, were reassigned to *Circus cyaneus*. Individual No. 564, initially classified as *Circus pygargus* was removed from the database after verifying that the specimen did not exist. Individual No. 576, initially classified as *Circus cyaneus*, was reclassified as *Circus aeruginosus*; however, it was removed from the database because there were insufficient bones for analysis. Finally, individual No. 744, initially classified as *Falco tinnunculus*, was identified as *Falco subbuteo* following confirmation of a sampling error.

Table 2
Names and numbers of individuals per species in the second database.

Scientific Name	Common Name	Individuals
Accipiter gentilis	Goshawk	34
Accipiter nisus	Sparrowhawk	34
Aegypius monachus	Cinereus vulture	49
Aquila adalberti	Imperial eagle	46
Aquila chrysaetos	Golden eagle	47
Aquila fasciata	Bonelli's eagle	60
Bubo bubo	Eagle owl	27
Buteo buteo	Common buzzard	34
Circaetus gallicus	Short-toed snake eagle	22
Circus aeruginosus	Western marsh harrier	31
Circus cyaneus	Hen harrier	11
Circus pygargus	Montagu's harrier	28
Elanus caerulus	Black-winged kite	15
Falco columbarius	Merlin	17
Falco naumanni	Lesser kestrel	27
Falco peregrinus	Peregrine falcon	33
Falco subbuteo	Eurasian hobby	26
Falco tinnunculus	Common kestrel	33
Gypaetus barbatus	Bearded vulture	15
Gyps fulvus	Griffon vulture	52
Hieraaetus pennatus	Booted eagle	34
Milvus migrans	Black kite	51
Milvus milvus	Red kite	38
Neophron percnopterus	Egyptian vulture	36
Pandion haliaetus	Osprey	24
Pernis apivorus	Honey buzzard	27
Total:		851

Therefore, two individuals were removed from the database, and the species classification of five others was reclassified. As a result, the database comprised 851 individuals from 26 species, each with 11 bone measurements from nine bones (Table 2).

3.2. Second prediction

After updating the database, a second estimation analysis was performed to complete the missing measurements for 377 individuals. A new database (Supplementary Table 3) was obtained, and a canonical discriminant analysis was performed again to determine species identity, this time examining the relationship among 11 bone measurements. A total of 11 linear functions of the following type were obtained:

$$\begin{aligned}\text{CVAi} = {} & \text{aiCxW CoxalW} + \text{aiCxL CoxalL} + \text{aiSkW SkullW} + \text{aiSkL SkullL} \\ & + \text{aiU Ulna} + \text{aiS Sternum} + \text{aiF Femur} + \text{aiH Humerus} \\ & + \text{aiR Radius} + \text{aiTm Tarsometatarsus} + \text{aiTt Tibiotarsus}\end{aligned}$$

where “W” is the width measurement and “L” is the length measurement.

There were no errors in species prediction, meaning the program correctly classified all individuals within the species defined in the original sampling.

3.3. Analysis of the relationship between bone measurements using a single data point: length

After performing a canonical discriminant analysis to compare the relationships between bone measurements for bones with only length data available (ulna, sternum, femur, humerus, tarsometatarsus, tibiotarsus, and radius). A total of 21 statistical models were obtained. Each model evaluated the relationship between the lengths of two bones. The linear functions obtained for each model were expressed as:

$$\text{CVA}_i = a_{i1}\, m_1 + a_{i2}\, m_2$$

where “m_1” y “m_2” represent the bone measurements being compared in each model.

After obtaining these models, cross-validation idendified the model with the highest species accuracy was the one relating the tarsometatarsus and ulna measurements, with an accuracy rate of 94.53%. The canonical discriminant plot for this best-performing two-bone model is provided in Fig. 4, illustrating the separation among species. In addition, the species-specific discriminant classification functions (equations) for this two-bone model are provided in Supplementary Material. The second-best model related the lengths of the tarsometatarsus and radius, with an accuracy rate of 94.05%. This was followed by the tarsometatarsus-humerus model (93.02%), then the tibiotarsus-humerus model (91.54%) (Table 3).

3.4. Analysis of the relationship between two measurements (width and length) and the rest of the bone measurements

Canonical discriminant analysis was performed to compare the synsacrum length and postacetabular ilium width and length and width of the skullbones with the measurements of the other bones. Fourteen statistical models were obtained, each analyzing the relationship between three bone measurements. The linear functions obtained were of the following form:

$$\text{CVA}_i = a_{i1}\, m_1 + a_{i2}\, m_2 + a_{i3}\, m_3$$

where “m_1” corresponds to the length and ‘m2’ corresponds to the width of the skull or pelvis. And “m_3” represents the length of another bone (ulna, sternum, femur, humerus, tarsometatarsus, tibiotarsus, or radius).

After obtaining all the models, cross-validation was conducted to

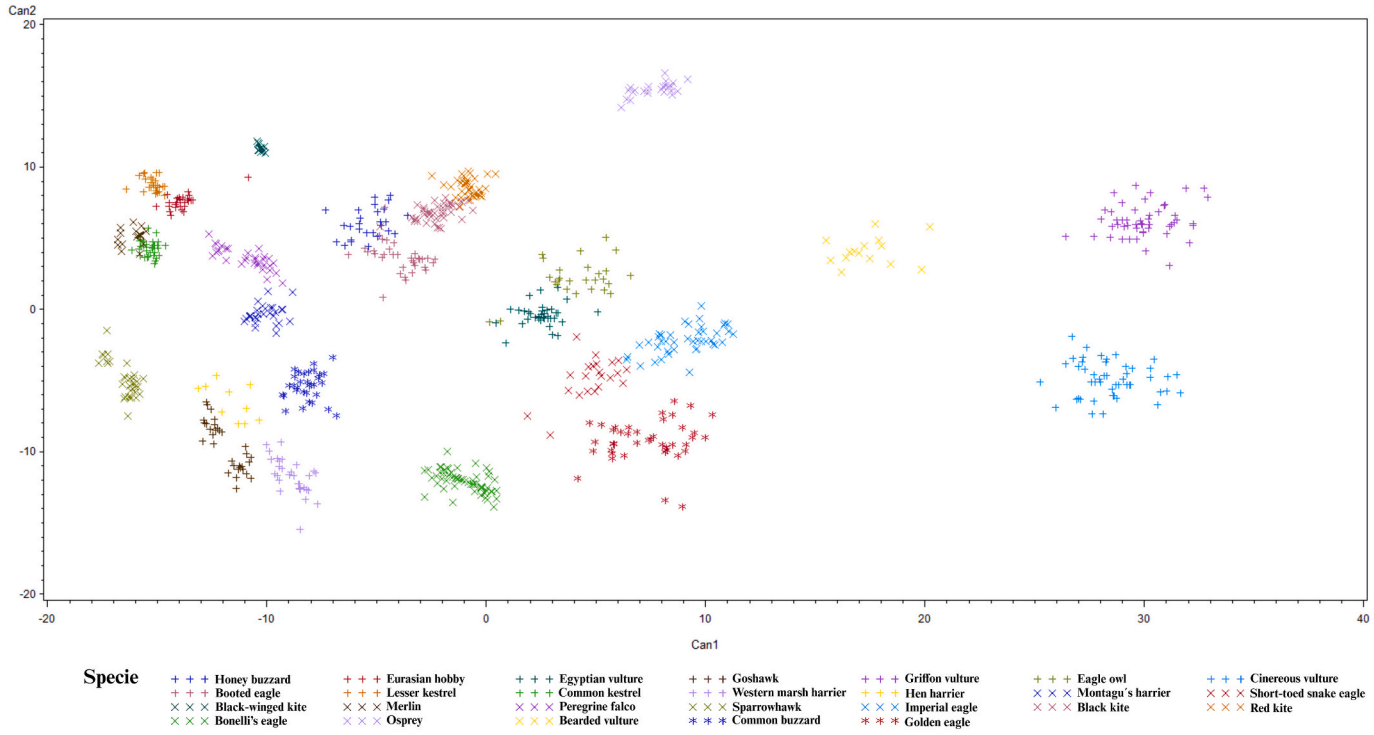

Fig. 4. Canonical discriminant analysis plot for the best-performing two-bone model based on tarsometatarsus length and ulna length. Points represent individual specimens.

Table 3
Results of cross-validation of bones with a single data point: length.

Bones	Error rate	% Error	% Accuracy
Tarsometatarsus and Ulna	0.0547	5.47	94,53
Tarsometatarsus and Radius	0.0595	5.95	94.05
Tarsometatarsus and Humerus	0.0698	6.98	93.02
Tibiotarsus and Humerus	0.0846	8.46	91.54
Femur and Radius	0.1000	10.00	90.00
Tibiotarsus and Ulna	0.1006	10.06	89.94
Femur and Ulna	0.1041	10.41	89.59
Tibiotarsus and Radius	0.1109	11.09	88.91
Femur and Humerus	0.1125	11.25	88.75
Tibiotarsus and Tarsometatarsus	0.1159	11.59	88.41
Femur and Tarsometatarsus	0.1306	13.06	86.94
Sternum and Tarsometatarsus	0.1317	13.17	86.83
Sternum and Tibiotarsus	0.1971	19.71	80.29
Sternum and Humerus	0.2261	22.61	77.39
Sternum and Radius	0.2356	23.56	76.44
Sternum and Ulna	0.2357	23.57	76.43
Femur and Tibiotarsus	0.2432	24.32	75.68
Sternum and Femur	0.2538	25.38	74.62
Humerus and Radius	0.2677	26.77	73.23
Humerus and Ulna	0.2937	29.37	70.63
Ulna and Radius	0.4368	43.68	56.32

"% Accuracy" percentage accuracy in species prediction. "% Error" percentage error in species prediction.

estimate error rates and accuracy percentages for species prediction, using the same approach as in the single-length analysis. The model combining the length and width of the pelvis with the length of the tarsometatarsus achieved the highest species prediction accuracy, at 91.48% (Table 4).

3.5. Analysis of the relationship between tarsometatarsus and ulna length with other bone measurements

After determining that the model combining tarsometatarsus and ulna lengths achieved the highest percentage of species accuracy (94.53%), a canonical discriminant analysis was performed to compare the relationship between the length of the tarsometatarsus and ulna to evaluate whether adding a third bone measurement could further improve prediction performance. Nine statistical models were obtained to analyze the relationship among three variables. The linear functions obtained were expressed as:

$$CVA_i = a_iC\ Ulna + a_iTM\ Tarsometatarsus + a_{i3}\ m_3$$

Table 4
Results of cross-validation for models combining the synsacrum length and postacetabular ilium width and length and width of the skull bones with the length of other bones.

Bone measurements	Error rate	% Error	% Accuracy
Synsacrum L Postacetabular ilium W and Tarsometatarsus	0.0852	8.52	91.48
Skull L, Skull W and Tarsometatarsus	0.1233	12.33	87.67
Synsacrum L Postacetabular ilium W and Ulna	0.1362	13.62	86.38
Synsacrum L Postacetabular ilium W and Radius	0.1424	14.24	85.76
Synsacrum L Postacetabular ilium W and Humerus	0.1572	15.72	84.28
Skull L Skull W and Tibiotarsus	0.1809	18.09	81.91
Synsacrum L Postacetabular ilium W and Tibiotarsus	0.1825	18.25	81.75
Skull L Skull W and Ulna	0.1865	18.65	81.35
Skull L Skull W and Radius	0.1886	18.86	81.14
Skull L Skull W and Femur	0.1921	19.21	80.79
Synsacrum L Postacetabular ilium W and Femur	0.2305	23.05	76.95
Synsacrum L Postacetabular ilium W and Sternum	0.2379	23.79	76.21
Skull L Skull W and Humerus	0.2477	24.77	75.23
Skull L Skull W and Sternum	0.2504	25.04	74.96

"W" width measurement. 'L' length measurement. "% Accuracy" percentage accuracy in species prediction. "% Error" percentage error in species prediction.

Table 5
Cross-validation results for tarsometatarsal and ulna length in relation to other bone measurements.

Bone measurements	Error rate	% Error	% Accuracy
Ulna, Tarsometatarsus, and Femur	0.0055	0.55	99.45
Ulna, Tarsometatarsus, and Sternum	0.0095	0.95	99.05
Ulna, Tarsometatarsus, and Tibiotarsus	0.0239	2.39	97.61
Ulna, Tarsometatarsus, and Postacetabular ilium W	0.0256	2.56	97.44
Ulna, Tarsometatarsus, and Synsacrum L	0.0337	3.37	96.63
Ulna, Tarsometatarsus, and Humerus	0.0377	3.77	96.23
Ulna, Tarsometatarsus, and Radius	0.0509	5.09	94.91
Ulna, Tarsometatarsus, and Skull W	0.0526	5.26	94.74
Ulna, Tarsometatarsus, and Skull L	0.0537	5.37	94.63

"W" width measurement. 'L' length measurement. "% Accuracy" percentage accuracy in species prediction. "% Error" percentage error in species prediction.

where "m_3" corresponds to any of the remaining bone measurements compared with the tarsometatarsus and ulna lengths.

Cross-validation of these models indicated that the combination of tarsometatarsus, ulna, and femur lengths exhibited the highest accuracy in predicting species, with 99.45% of classifications being correct (Table 5). The canonical discriminant plot for this best-performing three-bone model is shown in Fig. 5, displaying the distribution of individuals and the degree of separation among species. The species-specific discriminant classification functions (equations) for this three-bone model are also included in the Supplementary Material.

3.6. Verification of the bird identification method using bone measurements

The lengths of the tarsometatarsus and ulna were measured for each individual (Table 6), as this ratio yielded the highest percentage of successful species classification (94.53%).

A species prediction was made for each individual based on the results of a canonical discriminant analysis using these two measurements.

Table 6
Bone measurements obtained from radiographs.

ID	Length of tarsometatarsus (mm)	Length of ulna (mm)
1001	41.00	58.60
1002	39.60	60.40
1003	42.30	61.00
1004	43.00	61.00
1005	59.00	64.00
1006	52.00	58.00
1007	58.00	68.00
1008	58.00	66.00
1009	51.00	107.00
1010	52.00	108.00
1011	55.00	116.00
1012	44.00	78.00
1013	49.00	90.00
1014	45.00	79.00
1015	44.00	78.00

Most individuals were classified with an accuracy rate above 80%. Individuals 1005, 1006, 1007, and 1008 were classified with 100% probability as *Accipiter nisus* (Eurasian sparrowhawk) (Table 7). All predictions matched the actual species, yielding an overall classification accuracy of 100%.

4. Discussion

The results of this study support the initial hypothesis that the proposed standardized osteometric method is a suitable tool for identifying skeletal remains of birds of prey. This analysis enabled the identification of raptor species based on a combination of bone measurements from individual specimens. This method allows new skeletal findings to be classified with a high degree of accuracy by calculating probabilities of success and error.

Before performing statistical analysis, values for several individuals had to be estimated using multiple linear regression because the available measurements were limited to bone samples, leading to the random

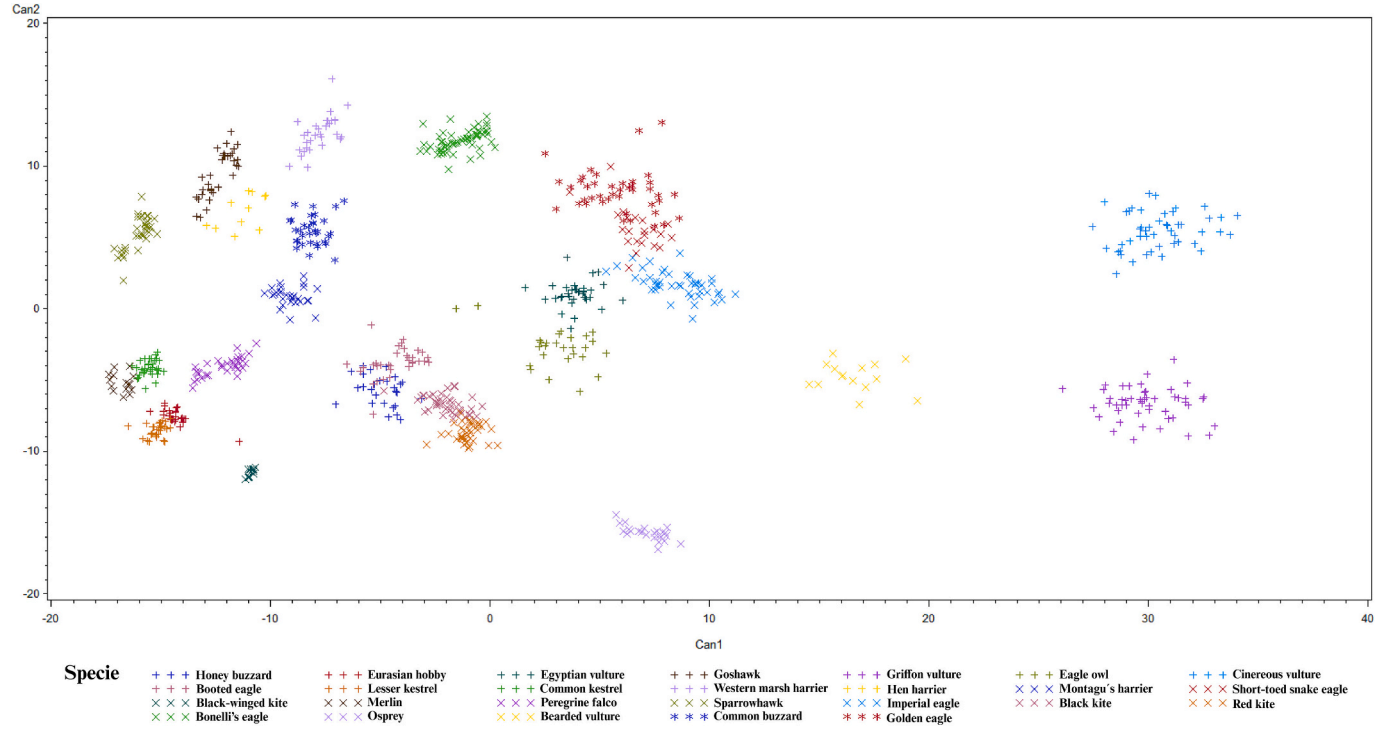

Fig. 5. Canonical discriminant analysis plot for the best-performing three-bone model based on tarsometatarsus length, ulna length and fémur length. Points represent individual specimens.

Table 7
Results of species identification based on bone measurements obtained from radiographs.

ID	Percentage of species assignment	Species prediction
1001	72.36%	*Falco tinnunculus*
1002	63.09%	*Falco tinnunculus*
1003	81.39%	*Falco tinnunculus*
1004	84.72%	*Falco tinnunculus*
1005	100.00%	*Accipiter nisus*
1006	100.00%	*Accipiter nisus*
1007	100.00%	*Accipiter nisus*
1008	100.00%	*Accipiter nisus*
1009	98.57%	*Pernis apivorus*
1010	96.57%	*Pernis apivorus*
1011	72.36%	*Pernis apivorus*
1012	93.37%	*Falco peregrinus*
1013	99.98%	*Falco peregrinus*
1014	97.06%	*Falco peregrinus*
1015	93.37%	*Falco peregrinus*

"Percentage of species membership" indicates the probability of belonging to the species assigned by the program. "Species prediction" refers to the species assigned to an individual by the program.

absence of specific skeletal elements. In the natural environment, regardless of the cause of death, postmortem disarticulation, scavenger activity, mechanical fragmentation, and the effects of water and wind often lead to small or fragile bones being broken or missing. Certain bones, such as the ulna and tarsometatarsus, are usually intact and more frequently recovered; however, this may vary depending on the size of the bird of prey. This pattern was reflected in the initial database, in which approximately 80% of specimens had ulna and tarsometatarsus measurements, while measurements from smaller or fragile bones were missing (García-Matarranz et al., 2013; Gardner et al., 2016; García-Matarranz, 2019).

Canonical discriminant analysis was used for classification, along with cross-validation procedures to evaluate the classification performance of the resulting canonical functions. This multivariate technique reduces dimensionality by maximizing between-group variation relative to within-group variation through linear combinations of variables. This allows observations to be placed in a lower-dimensional space that optimizes separation between categories (Lorbes Medina et al., 2014; Sorbolini et al., 2016). Cross-validation provided a more realistic estimate of the method's predictive performance by reducing the risk of overfitting and reinforcing its robustness and reproducibility. The usefulness of cross-validation in applied ornithology has been demonstrated in studies combining external biometrics and osteometric data, where correct classification rates and Wilks' lambda values support its effectiveness (Analla et al., 2022).

Osteometric analysis is characterized as a simple, straightforward, and cost-effective technique (García-Matarranz et al., 2013; Watson and Ledogar, 2019). Unlike non-metric identification, osteometry produces quantitative measurements that are more easily replicated and can be more readily compared through statistical analyses (Watson and Ledogar, 2019). The process involves authorized personnel recovering bone remains, cleaning them, and measuring them according to a standardized protocol that minimizes interobserver error. This protocol defines anatomical landmarks, requires repeating measurements, and records the quality of each sample (García-Matarranz, 2019). Basic training — such as that provided to national park staff or government security forces — allows for direct comparison of measurements with reference values and specific identifications, eliminating the need for specialist assistance, advanced equipment, or external laboratories. This approach significantly reduces costs and improves response times (García-Matarranz et al., 2013; Watson and Ledogar, 2019).

The high predictive accuracy achieved by combining tarsometatarsus and ulna measurements can be explained by the fact that these two bones represent complementary morphofunctional axes. The tarsometatarsus reflects the morphology of the locomotor system, prey capture, and control mechanisms. At the same time, the ulna describes the wing's structure and its relationship to flight style, such as maneuvering and gliding (Corvidae et al., 2006). Together, these bones integrate body size and proportion elements in nearly orthogonal directions, reducing collinearity and maximizing interspecific variance. This improves canonical separation and reduces the classification error among raptor species. Additionally, both bones are easily accessible and identifiable by their morphological characteristics, which would facilitate their use in analyses by non-specialized personnel (García-Matarranz, 2019). Although this combination had the highest accuracy, the inclusion of the tarsometatarsus in other combinations suggests that interspecific differences may be more related to feeding strategy than flight type. These results indicate that hunting and feeding behavior (aerial, terrestrial, or aquatic) and the ecological niche may influence the development of tarsometatarsal morphology (Zeffer et al., 2003; Carril et al., 2024). The combination of tarsometatarsus, ulna, and femur measurements achieved the highest overall accuracy. However, verification of the method using radiograph was limited to the first two bones to demonstrate that high predictive power can be maintained with minimal skeletal data. This dramatically enhances the method's applicability in cases involving incomplete remains (Watson and Ledogar, 2019).

Alternative methods require greater resource investment and specialized expertise. Examples include body biometrics for sex determination in sexually dysmorphic species (Delgado and Penteriani, 2004; Muriel et al., 2010; García-Matarranz et al., 2013; García et al., 2021) and blood and genetic analyses (Muriel et al., 2010). In contrast, osteometry prioritizes the use of affordable tools such as calipers and includes simple quality controls, including periodic calibration, duplicate measurements, and resolution of discrepancies (García-Matarranz et al., 2013; García-Matarranz, 2019). In our study, the reference database was constructed from direct bone measurements, while radiographs were used solely to verify that the model's performance is transferable to imaging when the same anatomical landmarks and scale are applied. Operationally, bone analysis reduces response times in the field, lowers logistical costs, and reserves complementary techniques, such as DNA sequencing, for when they are essential, for example, with highly fragmented samples, species that are difficult to identify, or forensic/judicial applications (Muriel et al., 2010).

Routinely adopting this approach would facilitate population monitoring and assessment of the anthropogenic impacts, such as collisions, electrocutions, lead poisoning, and illegal baiting. Rapid and traceable identification would also enable the implementation of more effective conservation strategies (Berny et al., 2015; Descalzo et al., 2021; Estellés-Domingo and López-López, 2025; O'Bryan et al., 2022; Rial-Berriel et al., 2021; Vyas et al., 2022). In addition, the practical applicability of the method has already been demonstrated both in real-world cases involving birds of prey and in the radiographs, as verified in this study. This strengthens its potential for use in wildlife management, scientific research, or forensic contexts, where standardizing measurements and using photographic documentation provides additional reliability and reproducibility (García-Matarranz et al., 2013; García-Matarranz, 2019).

However, this study has certain limitations. The database includes only raptor species present in Spain, limiting extrapolation to other biogeographical regions. Additionally, the sex of the individuals was not considered, which could introduce intraspecific variability due to sexual size dimorphism. This means that sexing tests must be based on DNA samples, which is sometimes economically unfeasible. Future studies should aim to analyze and incorporate sex and age metadata wherever possible. Extrapolation to other avian groups, such as migratory passerines, may also be limited by morphofunctional differences between resident and migratory populations, including differences in the sternum, humerus, or tibiotarsus associated with lifestyle (Singh et al., 2015). Although the results are highly reliable, some margin of error can

be expected due to the condition of the remains and measurement precision. In context requiring unequivocal identification, the proposed osteometric approach can be supplemented with DNA sequencing or other diagnostic methods. These findings could be further developed using machine learning to optimize classification and external validation, and to integrate radiographic or photographic data to create increasingly reliable and advanced predictive models. This would minimize measurement errors, accelerate data processing, and facilitate the development of user-friendly applications, enabling competent authorities and wildlife recovery centres to utilise the method without requiring advanced training. Future studies should evaluate combinations in non-Iberian raptors and assess applicability in non-raptor species to test the phylogenetic validity and define the taxonomic scope of the method.

In conclusion, this study has established an osteometric database comprising 26 raptor species with 11 measurements taken from nine bones. Canonical discriminant analysis demonstrated that combining tarsometatarsus and ulna measurements achieves 94.53% accuracy, increasing to 99.45% when the femur is included. Furthermore, verifying the methodology with individuals outside the database confirmed a predictive capacity of nearly 100%, demonstrating the approach's applicability in specifically identifying birds of prey from skeletal remains. The proposed osteometric identification method could be implemented in the Ministry of Ecological Transition, as well as for technicians, state security forces, national natural parks, and recovery centres throughout Spain. This will contribute to the practical conservation and monitoring of raptor populations. In the future, inclusion of other species, sexes, ages, and populations will be necessary, as will field evaluations with different observers and external teams to estimate the method's reproducibility and robustness across geographical variation, and to improve it through machine learning and predictive models.

Supplementary data to this article can be found online at https://doi.org/10.1016/j.rvsc.2026.106121.

Animal ethic statement

No Animal Ethics Statement was required for this study, as no animals were used.

CRediT authorship contribution statement

Andrea Miguel-Batuecas: Writing – review & editing, Writing – original draft, Methodology, Investigation, Formal analysis, Conceptualization. **Juan A. De Pablo-Moreno:** Writing – review & editing, Writing – original draft, Methodology, Investigation, Formal analysis, Data curation, Conceptualization. **Manuel Fuertes-Recuero:** Writing – review & editing, Writing – original draft, Investigation, Formal analysis, Conceptualization. **Ariana Fuentes-Díaz:** Writing – review & editing, Methodology, Investigation, Formal analysis, Data curation, Conceptualization. **Fernando González:** Writing – review & editing, Methodology, Investigation, Funding acquisition, Conceptualization. **Laura Suárez:** Writing – review & editing, Methodology, Investigation, Conceptualization. **Victoriano García-Matarranz:** Writing – review & editing, Supervision, Methodology, Investigation, Formal analysis, Data curation. **Luis Revuelta:** Writing – review & editing, Project administration, Methodology, Investigation, Funding acquisition, Formal analysis, Data curation, Conceptualization.

Declaration of generative AI and AI-assisted technologies in the writing process

No generative AI or AI-assisted technologies were used in the writing process.

Funding source

This work received funding from the Directorate-General for Biodiversity, Forests and Desertification of Spain's Ministry for the Ecological Transition and the Demographic Challenge (contract 21BDMC011), as part of efforts to protect avifauna from collision and electrocution on high-voltage power lines.

Declaration of competing interest

The authors declare the following financial interests/personal relationships which may be considered as potential competing interests. Luis Revuelta has patent “Base de Datos de Reconocimiento de Aves Rapaces por medidas de huesos BDRARH,” with reference number M-004841/2021 licensed to Licensee. Victoriano Garcia-Matarranz has patent #Base de Datos de Reconocimiento de Aves Rapaces por medidas de huesos BDRARH,” with reference number M-004841/2021 licensed to Licensee. If there are other authors, they declare that they have no known competing financial interests or personal relationships that could have appeared to influence the work reported in this paper.

Acknowledgments

All statistical analyses were performed with the assistance of the Administrative Network Technical User Support (ATU) department. The authors acknowledge the financial support provided by the Ministry for Ecological Transition and the Demographic Challenge but do not express the opinion of the Ministry. The authors thank their institutions for supporting this project. The authors would like to thank Andreia Dias for her assistance with the handling of bone samples.

Data availability

All data supporting the findings of this study are included in the manuscript and its supplementary material. Additional information is available from the corresponding author upon reasonable request.

References

Analla, M., Fernández-Rodríguez, P., Martínez-Medina, N., Azorit, C., 2022. Sexing Eurasian Eagle Owls by external body and skeletal measurements. J. Field Ornithol. 93, 1. https://doi.org/10.5751/JFO-00175-930401.

Berny, P., Vilagines, L., Cugnasse, J.-M., Mastain, O., Chollet, J.-Y., Joncour, G., Razin, M., 2015. VIGILANCE POISON: illegal poisoning and lead intoxication are the main factors affecting avian scavenger survival in the Pyrenees (France). Ecotoxicol. Environ. Saf. 118, 71–82. https://doi.org/10.1016/j.ecoenv.2015.04.003.

Buechley, E.R., Şekercioğlu, Ç.H., 2016. The avian scavenger crisis: looming extinctions, trophic cascades, and loss of critical ecosystem functions. Biol. Conserv. 198, 220–228. https://doi.org/10.1016/j.biocon.2016.04.001.

Carril, J., De Mendoza, R.S., Degrange, F.J., Barbeito, C.G., Tambussi, C.P., 2024. Evolution of avian foot morphology through anatomical network analysis. Nat. Commun. 15, 9888. https://doi.org/10.1038/s41467-024-54297-9.

Corvidae, E., Bierregaard, R., Peters, S., 2006. Comparison of wing morphology in three birds of prey: correlations with differences in flight behavior. In: J. Morphol., 267, pp. 612–622. https://doi.org/10.1002/jmor.10425.

Dalén, L., Lagerholm, V.K., Nylander, J.A.A., Barton, N., Bochenski, Z.M., Tomek, T., Rudling, D., Ericson, P.G.P., Irestedt, M., Stewart, J.R., 2017. Identifying bird remains using ancient DNA barcoding. Genes 8, 169. https://doi.org/10.3390/genes8060169.

Delgado, M., Penteriani, V., 2004. Gender determination of Eurasian eagle-owls (*Bubo bubo*) by morphology. J. Raptor Res. 38.

Descalzo, E., Camarero, P.R., Sánchez-Barbudo, I.S., Martinez-Haro, M., Ortiz-Santaliestra, M.E., Moreno-Opo, R., Mateo, R., 2021. Integrating active and passive monitoring to assess sublethal effects and mortality from lead poisoning in birds of prey. Sci. Total Environ. 750, 142260. https://doi.org/10.1016/j.scitotenv.2020.142260.

Donázar, J.A., Cortés-Avizanda, A., Fargallo, J.A., Margalida, A., Moleón, M., Morales-Reyes, Z., Moreno-Opo, R., Pérez-García, J.M., Sánchez-Zapata, J.A., Zuberogoitia, I., Serrano, D., 2016. Roles of raptors in a changing world: from flagships to providers of key ecosystem services. Ardeola 63, 181–234. https://doi.org/10.13157/arla.63.1.2016.rp8.

Dwyer, J.F., Harness, R.E., Gerber, B.D., Landon, M.A., Petersen, P., Austin, D.D., Woodbridge, B., Williams, G.E., Eccleston, D., 2016. Power pole density informs

spatial prioritization for mitigating avian electrocution. J. Wildl. Manag. 80, 634–642. https://doi.org/10.1002/jwmg.1048.
Eccleston, D.T., Harness, R.E., 2018. Raptor electrocutions and power line collisions. In: Sarasola, J.H., Grande, J.M., Negro, J.J. (Eds.), Birds of Prey. Springer, Cham, pp. 273–302. https://doi.org/10.1007/978-3-319-73745-4_12.
Estellés-Domingo, I., López-López, P., 2025. Effects of wind farms on raptors: a systematic review of the current knowledge and the potential solutions to mitigate negative impacts. Anim. Conserv. 28, 334–352. https://doi.org/10.1111/acv.12988.
García, J., Arizaga, J., Rodríguez, J.I., Alonso, D., Suárez-Seoane, S., 2021. Morphological differentiation in a migratory bird across geographic gradients in mountains of southern Europe. J. Biogeogr. 48, 2828–2838. https://doi.org/10.1111/jbi.14242.
García-Matarranz, V., 2019. Guía de identificación de rapaces ibéricas por restos óseos. Available in: https://www.miteco.gob.es/content/dam/miteco/es/biodiversidad/temas/conservacion-de-especies/guiarapacesrestososeos1parte_tcm30-198046.pdf.
García-Matarranz, V., Moreno-Opo, R., Tintó, A., 2013. Sex differentiation of Bonelli's Eagle Aquila fasciata in Western Europe using morphometrics and plumage colour patterns. Ardeola 60, 261–277. https://doi.org/10.13157/arla.60.2.2013.261.
Gardner, E.E., Walker, S.E., Gardner, L.I., 2016. Palaeoclimate, environmental factors, and bird body size: a multivariable analysis of avian fossil preservation. Earth Sci. Rev. 162, 177–197. https://doi.org/10.1016/j.earscirev.2016.07.001.
Gómez-Catasús, J., Carrascal, L.M., Moraleda, V., Colsa, J., Garcés, F., Schuster, C., 2020. Factors affecting differential underestimates of bird collision fatalities at electric lines: a case study in the Canary Islands. Ardeola 68, 71. https://doi.org/10.13157/arla.68.1.2021.ra5.
Gorobets, L., Volynskyi, T., Kovalchuk, O., 2024. Birds of prey in the historical past of Eastern Europe: evidence from bones. J. Archaeol. Sci. Rep. 58, 104735. https://doi.org/10.1016/j.jasrep.2024.104735.
Guil, F., Pérez-García, J.M., 2022. Bird electrocution on power lines: spatial gaps and identification of driving factors at global scales. J. Environ. Manage. 301, 113890. https://doi.org/10.1016/j.jenvman.2021.113890.
Katzner, T.E., Pain, D.J., McTee, M., Brown, L., Cuadros, S., Pokras, M., Slabe, V.A., Watson, R.T., Wiemeyer, G., Bedrosian, B., Hampton, J.O., Parish, C.N., Pay, J.M., Saito, K., Schulz, J.H., 2024. Lead poisoning of raptors: state of the science and cross-discipline mitigation options for a global problem. Biol. Rev. 99, 1672–1699. https://doi.org/10.1111/brv.13087.
Komosa, M., Włodarek, J., Frąckowiak, H., Zdun, M., Charuta, A., Gogulski, M., Mizera, T., 2018. Osseous pathological changes in the white-tailed eagle (Haliaeetus albicilla) in its central European habitat. Pol. J. Environ. Stud. 28, 701–708. https://doi.org/10.15244/pjoes/85223.
Lorbes Medina, J., Garcia Orellana, Y., Milla Pino, M., Diaz, L., 2014. Análisis discriminante canónico con técnicas gráficas multivariadas aplicado a un diseño con dos factores. Adv. Investig. Ing. 11, 38–47. https://doi.org/10.18041/1794-4953/avances.2.227.
McClure, C.J.W., Westrip, J.R.S., Johnson, J.A., Schulwitz, S.E., Virani, M.Z., Davies, R., Symes, A., Wheatley, H., Thorstrom, R., Amar, A., Buij, R., Jones, V.R., Williams, N. P., Buechley, E.R., Butchart, S.H.M., 2018. State of the world's raptors: distributions, threats, and conservation recommendations. Biol. Conserv. 227, 390–402. https://doi.org/10.1016/j.biocon.2018.08.012.
McClure, C.J.W., Dunn, L., Buechley, E.R., Juergens, P., Oleyar, D., Goodrich, L.J., Therrien, J.-F., 2022. Conservation assessment of raptors within the USA and Canada. Biol. Conserv. 272, 109633. https://doi.org/10.1016/j.biocon.2022.109633.
McClure, C.J.W., Buij, R., Thorstrom, R., Vargas, F.H., Virani, M.Z., 2023. The world's most imperiled raptors present substantial conservation challenges. J. Raptor Res. 57 (3), —. https://doi.org/10.3356/JRR-22-79.
Muriel, R., Casado, E., Schmidt-Rothmund, D., Calabuig, C., Ferrer, M., 2010. Morphometric sex determination of young ospreys Pandion haliaetus using discriminant analysis. Bird Study 57, 336–343. https://doi.org/10.1080/00063651003674953.
O'Bryan, C.J., Allan, J.R., Suarez-Castro, A.F., Delsen, D.M., Buij, R., McClure, C.J.W., Rehbein, J.A., Virani, M.Z., McCabe, J.D., Tyrrell, P., Negret, P.J., Greig, C., Brehony, P., Kissling, W.D., 2022. Human impacts on the world's raptors. Front. Ecol. Evol. 10, 624896. https://doi.org/10.3389/fevo.2022.624896.
Rial-Berriel, C., Acosta-Dacal, A., Cabrera Pérez, M.Á., Suárez-Pérez, A., Melián Melián, A., Zumbado, M., Henríquez Hernández, L.A., Ruiz-Suárez, N., Rodriguez Hernández, Á., Boada, L.D., Macías Montes, A., Luzardo, O.P., 2021. Intensive livestock farming as a major determinant of the exposure to anticoagulant rodenticides in raptors of the Canary Islands (Spain). Sci. Total Environ. 768, 144386. https://doi.org/10.1016/j.scitotenv.2020.144386.
Santangeli, A., Girardello, M., 2021. The representation potential of raptors for globally important nature conservation areas. Ecol. Indic. 124, 107434. https://doi.org/10.1016/j.ecolind.2021.107434.
Sarasola, J.H., Grande, J.M., Negro, J.J., 2018. Birds of Prey. Springer, Cham. https://doi.org/10.1007/978-3-319-73745-4.
Singh, N.S., Bamon, I., Dixit, A.S., Sougrakpam, R., 2015. Structural variations and their adaptive significances in the bones of some migratory and resident birds. J. Basic Appl. Zool. 70, 33–40. https://doi.org/10.1016/j.jobaz.2015.06.003.
Sorbolini, S., Gaspa, G., Steri, R., Dimauro, C., Cellesi, M., Stella, A., Marras, G., Marsan, P.A., Valentini, A., Macciotta, N.P.P., 2016. Use of canonical discriminant analysis to study signatures of selection in cattle. Genet. Sel. Evol. 48, 58. https://doi.org/10.1186/s12711-016-0236-7.
Tincher, M.C., Dwyer, J.F., Kratz, G.E., Watrud, A., Harness, R.E., 2020. Perch management may reduce raptor electrocution risk on horizontal post insulators. J. Raptor Res. 54, 186. https://doi.org/10.3356/0892-1016-54.2.186.
Vidaña, B., Busquets, N., Napp, S., Pérez-Ramírez, E., Jiménez-Clavero, M.Á., Johnson, N., 2020. The role of birds of prey in West Nile virus epidemiology. Vaccines 8, 550. https://doi.org/10.3390/vaccines8030550.
Vyas, N.B., Rattner, B.A., Lockhart, J.M., Hulse, C.S., Rice, C.P., Kuncir, F., Kritz, K., 2022. Toxicological responses to sublethal anticoagulant rodenticide exposure in free-flying hawks. Environ. Sci. Pollut. Res. Int. 29, 74024–74037. https://doi.org/10.1007/s11356-022-20881-z.
Watson, J.E., Ledogar, S.H., 2019. Testing the effectiveness of osteometrics in the identification of North American gallinaceous bird post-cranial elements. Archaeol. Anthropol. Sci. 11, 2623–2636. https://doi.org/10.1007/s12520-018-0697-4.
Woodward, A.M., 2023. Morphometrics as a tool for the species identification of North American Bald and Golden Eagle primary feathers. J. Raptor Res. 57 (3), —. https://doi.org/10.3356/JRR-22-01.
Zeffer, A., Johansson, L.C., Marmebro, Å., 2003. Functional correlation between habitat use and leg morphology in birds (Aves). Biol. J. Linn. Soc. 79, 461–484. https://doi.org/10.1046/j.1095-8312.2003.00200.x.